Journal of Controlled Release 247 (2017) 64–72

Contents lists available at ScienceDirect

Journal of Controlled Release

journal homepage: www.elsevier.com/locate/jconrel

Inhomogeneous crystal grain formation in DPPC-DSPC based thermosensitive liposomes determines content release kinetics

Tao Lu *, Timo L.M. ten Hagen **,[1]

Laboratory Experimental Surgical Oncology, Section Surgical Oncology, Department of Surgery, Erasmus MC, Rotterdam, The Netherlands

ARTICLE INFO

Article history:
Received 2 October 2016
Received in revised form 9 December 2016
Accepted 16 December 2016
Available online 29 December 2016

Chemical compounds studied in this article:
DPPC (PubChem CID: 160339)
DSPC (PubChem CID: 94190)
DSPE-PEG (PubChem CID: 86278269)
Carboxyfluorescein (PubChem CID: 123755)
Cholesterol (PubChem CID: 5997)
HEPES (PubChem CID: 23,831)

Keywords:
Thermosensitive liposome
DPPC
DSPC
Inhomogeneous crystal grain
Phase transition
Release kinetics

ABSTRACT

Thermosensitive liposomes (TSL) receive attention due to their rapid externally controlled drug release at transition temperature in combination with hyperthermia. This rapid release feature of TSL occurs when the liposome membrane is going through a phase change which results in numerous interfaces, at so-called crystal grain boundaries. Based on experience with TSLs, our group found that thermosensitive liposomes formulated by binary compositions of DPPC and DSPC at proper ratios are able to exhibit rapid release without incorporation of release-promoting components. The aim of this study was to understand the mechanism of rapid release from bi-component DPPC-DSPC based TSL. Based on the investigation of a series of TSLs formulated by different DPPC-DSPC ratios, and through the analysis of binary-phase diagrams of DPPC-DSPC TSLs, we conclude that inhomogeneous crystal grains are formed in bi-component TSL membranes rather than mono-component, thereby facilitating content release. The resulting inhomogeneous membrane pattern is affected by DPPC/DSPC ratio, i.e. this determines the number of interfaces between solid and liquid phases at transition temperature, which can be diminished by addition of cholesterol. At appropriate DPPC/DSPC ratio, substantive solid/liquid interfaces can be generated not only between membrane domains but also between crystal grains in each domain of the liposome membranes, therefore improving content release from the TSL at transition temperatures.

1. Introduction

Nanoparticle-mediated chemotherapy offers several advantages in tumor treatment, including reduced side-effects, prolonged circulation time and possibly improved intratumoral drug accumulation due to the enhanced permeability and retention (EPR) effect [1]. Especially lipid-based particles, liposomes, are successfully developed of which Doxil®/Caelyx® is one of most well-known and widely used. However, application of nanoparticles also introduces drawbacks, such as failure to adequately penetrate tumors [2]. The EPR effect is influenced by tumor microenvironment, tumor type and profile of nanoparticle, which all may hinder an optimal therapeutic effect of most conventional, passively-delivered liposomal formulations [3,4]. Important, and the key explanation for failure of Doxil® to surpass doxorubicin, is the slow drug release from the liposome, which limits therapeutic efficacy in spite of strikingly increased circulation time [5]. Hence, to obtain high local levels of free and bioavailable drug actively triggered release of encapsulated drug at the diseased site is a pursued possibility. One approach for local delivery is to use thermosensitive liposomes (TSL) and local hyperthermia (HT), in which the drug is rapid intravascularly released in the heated area, subsequently followed by massive uptake by tumor cells due to high concentration gradients.

The concept of thermosensitive liposomes was first introduced by Yatvin et al. [6], reporting a TSL formed by 1,2-dipalmitoyl-sn-glycero-3-phosphocholine (DPPC) alone or with 1,2-distearoyl-sn-glycero-3-phosphocholine (DSPC), which generates content release at a phase transition temperature around 42 °C. Nevertheless, these TSL relatively slowly release their content limiting further application [7]. To enhance release from TSL, Needham et al. improved TSL composition by

* Correspondence to: T. Lu, Laboratory Experimental Surgical Oncology, Section Surgical Oncology, Department of Surgery, Erasmus MC, Room Ee175, 3000CA Rotterdam, PO Box 1738, 3000 DR Rotterdam, The Netherlands.
** Correspondence to: T. L.M. ten Hagen, Laboratory Experimental Surgical Oncology, Section Surgical Oncology, Department of Surgery, Erasmus MC, Room Ee 0104a, PO Box 1738, 3000 DR Rotterdam, The Netherlands.
E-mail addresses: t.lu@erasmusmc.nl (T. Lu), t.l.m.tenhagen@erasmusmc.nl (T.L.M. ten Hagen).
[1] Dr. Molewaterplein 50, 3015 GE Rotterdam.

http://dx.doi.org/10.1016/j.jconrel.2016.12.030

incorporating lysolipid (LPC) and 1,2-distearoyl-sn-glycero-3-phosphoethanolamine-N-methoxy(PEG)-2000 (DSPE-PEG2000) in DPPC-based formulations. These LPC-containing TSLs show over 80% release in a matter of seconds at around 41 °C, achieving a rapid release profile necessary for intravascular delivery [8,9]. Currently, several different thermosensitive liposomal formulations have been reported [10].

The principle of TSL release is generally thought to result from phase separation at Tm causing interfaces or gaps in the bilayer enabling content release [10]. Ickenstein et al. proposed that lipids solidify into gel-phase domains in the membrane during cooling, and boundaries appear at adjacent domains due to spherical bending force [11]. Because of a high degree of disordered lipid-arrangement in domain boundaries, these regions possess lower melting points. This causes prior phase transition at domain boundaries, thus generating interfaces between gel/liquid-crystalline phases, which are in turn responsible for release of content [11,12]. Surfactant lysolipids tend to migrate to phase interfaces and form micelle-structures at phase transition, thus inducing nano-pores in membranes, which can be stabilized by PEG-linked lipids. Together they increase and enlarge the interfaces inflicting more rapid release [9,13]. Based on the same principle, Tagami et al. added Brij surfactants into DPPC-based TSL, which exerts comparable fast release in response to hyperthermia [14].

Most thermosensitive liposomes are formulated on the initially proposed matrix composed of DPPC and DSPC phospholipids [15–18]. Especially, in our group we have been working on DPPC-DSPC based thermosensitive liposomes for years and developed several PEG-DSPE-modified DPPC-DSPC based TSLs loaded with different drugs, showing desired temperature response [19–22]. In the follow-up study, we observed that TSLs formulated at proper DPPC/DSPC ratios exhibit rapid release at transition temperatures. However, this fast release is likely not explained by the defect mechanism of Ickenstein [11], and does not result from the nano-pore effect seen with lysolipid-based TSL as proposed by Needham et al. [9]. We speculate that apart from boundaries between individual domains as defective regions in membranes, other release regions and factors exist that influence content release from DPPC-DSPC based TSLs at transition temperatures. Therefore, in this study we designed DPPC-DSPC based TSLs, investigated rapid release at certain DPPC/DSPC ratios during phase transition, and elucidated the principle to achieve an optimal heat-triggered release DPPC-DSPC based liposome system.

2. Materials and methods

2.1. Chemicals and agents

1,2-Dipalmitoyl-sn-glycero-3-phosphcholine (DPPC), 1,2-distearoyl-sn-glycero-3-phosphocholine (DSPC) and 1,2-distearoyl-sn-glycero-3-phosphoethanolamine-N-PEG_{2000} (DSPE-PEG) were provided by Lipoid (Ludwigshafen, Germany). Purified carboxyfluorescein (CF) was kindly provided by Dr. Lars Lindner and colleagues. PD-10 columns were obtained from GE Healthcare (UK). Cholesterol and other chemicals were purchased from Sigma Aldrich unless otherwise specified.

2.2. Preparation of liposomes

TSLs were composed of DPPC/DSPC/DSPE-PEG in a molar ratio of x / (100 − x) / 5 (x = 100, 80, 60, 40, 20, 0) by using the thin lipid film hydration method, followed by heated extrusion [19]. Briefly, 100 μmol of lipids was dissolved in methanol/chloroform (1/9 v/v) mixed solvent which was then evaporated at 40 °C, followed by nitrogen flush for 30 min to remove residual solvent. The resulting dried lipid film was hydrated with CF (100 mM, pH 7.4) solutions at 60 °C. Small unilamellar vesicles were obtained by extrusion through Nuclepore® (Whatman Inc., USA) filters with pore size of 100 nm on a Thermobarrel extruder at 65 °C (Northern Lipids, Canada). Unencapsulated CF was removed with a PD-10 column. Diameter (*Z*-average) and polydispersity index (PDI) were measured by using Zetasizer Nano-ZS (Malvern Instruments Ltd., UK).

2.3. Differential scanning calorimetry

Determination of TSL phase transition temperatures was done through differential scanning calorimetry (DSC) (NETZSCH Scientific Instruments Ltd. DSC200F). Six DPPC-DSPC based formulations were prepared as mentioned in Section 2.1 with or without CF loading. 30 mg of liposome with/without encapsulated CF in fetal calf serum (FCS) or in HEPES solution (pH 7.4), and the appropriate reference solution (HEPES solution), were added to the sealed aluminum container. The phase transition temperature range was measured over a temperature range of 30 to 70 °C at an interval of 5 °C/min increase. High purity nitrogen was used as carrier gas at rate of 10 ml/min.

2.4. CF-loaded TSL time- and temperature-dependent release

20 μl of 1 mM [lipid] CF-TSL suspension was added to 2 ml 100% FCS in a quartz cuvette at a series of determined temperature for 10 min. Real-time release of CF was detected with a water bath combined spectrofluorimetry (Ex. 493 nm/Em. 517 nm, Ex. slit 5 nm/Em. slit 5 nm) (Hitachi F-4500 Fluorescence Spectrophotometer, Japan). The average fluorescence intensity of the initial 5 s was recorded as I_0 of CF-TSL release, while fluorescence was measured as I_t at 10 min. After 10 min, detergent (10% Triton X-100) was used to disrupt all liposomes to measure maximal CF fluorescence, which was recorded as I_{max}. Release (%) = $(I_t - I_0) / (I_{max} - I_0) \times 100$.

2.5. Thermokinetic release of CF-loaded TSL

Time-dependent CF release curves obtained from Section 2.4, were fitted using three most common kinetic models (which are zero order, first order and Higuchi equations, respectively, see below), to determine the best-fitting profile of release kinetics and corresponding release rate [23].

$$\text{Zero order}: M_{t.} = M_0 + k_0\, t$$

$$\text{First order}: \ln(1 - M_t) = M_0 - k_1\, t$$

$$\text{Higuchi}: M_{t.} = M_0 + k_h t^{1/2}$$

where M_t is the amount of content released at time t. M_0 is the initial amount of release at time = 0. k_0, k_1 and k_h represent the release rate constant of zero-order, first-order and Higuchi, respectively. Here, M_t

Table 1
Characterization parameters of DPPC-DSPC based CF TSLs. Mean ± SD, $N \geq 3$.

TSL composition (mole)	Particle size (nm) (*Z*-average)[a]	Polydispersity index
DPPC/DSPE-PEG 100/5 (TSL 100)	117 ± 5	0.07 ± 0.01
DPPC/DSPC/DSPE-PEG 80/20/5 (TSL 80)	119 ± 3	0.05 ± 0.03
DPPC/DSPC/DSPE-PEG 60/40/5 (TSL 60)	113 ± 2	0.07 ± 0.02
DPPC/DSPC/DSPE-PEG 40/60/5 (TSL 40)	120 ± 4	0.04 ± 0.01
DPPC/DSPC/DSPE-PEG 20/80/5 (TSL 20)	115 ± 3	0.05 ± 0.02
DSPC/DSPE-PEG 100/5 (TSL 0)	119 ± 6	0.06 ± 0.02

[a] The *Z*-average of particle was reported by Zetasizer, which was measured based on Comulant model.

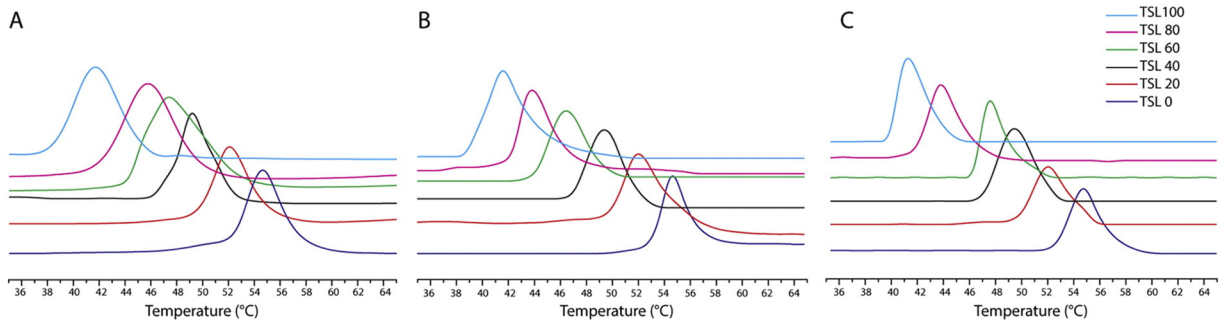

Fig. 1. DSC scans of empty liposome in HEPES (A), CF-loaded liposomes in HEPES (B) or in FCS (C). TSL100–0 represent liposomes formulated at (100/5:DPPC/PEG), (80/20/5:DPPC/DSPC/PEG), (60/40/5:DPPC/DSPC/PEG), (40/60/5:DPPC/DSPC/PEG), (20/80/5:DPPC/DSPC/PEG) and (100/5:DSPC/PEG), respectively.

represents the percentage CF released at time t, which was recorded based on CF fluorescence intensity.

2.6. Activation energy of CF release

Activation energy (Ea) of CF release from TSLs composed of different DPPC and DSPC ratios can be calculated by using Arrhenius indefinite integral equation:

$$\ln k = -(Ea/R) * (1/T) + B$$

where k is the CF release rate constant which can be obtained based on methods mentioned in Section 2.5, B is a constant, R is the universal gas constant, and T is expressed as thermodynamic temperature in Kelvin.

2.7. Statistical analysis

Data were analyzed using Mann-Whitney *U* test or Kruskal-Wallis test followed by Dunn test when appropriate. *p*-Values below 0.05 were considered significant.

3. Results

3.1. Differential scanning calorimetry

DPPC-DSPC based liposome formulations with or without encapsulated CF were prepared with diameters between 110 and 120 nm and PDI below 0.1 (Table 1). Liposomes were measured in FCS and HEPES buffer solution by DSC, respectively. As seen in Fig. 1, Tm increased with increasing DSPC content in the liposomal composition. Only one phase transition peak was observed with each formulation and the Tm was between those for pure DPPC and pure DSPC liposomes. These data suggest that a molecular dispersion system (solid solution) was achieved in DPPC-DSPC mixed lipid membranes. By comparison, when CF was encapsulated, liposomal Tm did not show significant changes in HEPES or FCS solution (Table 2).

Table 2
DPPC-DSPC liposome phase transition temperature.

Lipid composition	Internal solution	External solution	Phase transition temperature	Initial temperature of phase transition	Terminal temperature of phase transition
100% DPPC (TSL 100)	HEPES	HEPES	41.7	38.7	45.4
	CF	HEPES	41.0	40.4	43.2
		FCS	41.1	40.4	43.4
80% DPPC (TSL 80)	HEPES	HEPES	43.9	41.1	47.0
	CF	HEPES	43.7	42.5	45.9
		FCS	43.6	42.4	45.5
60% DPPC (TSL 60)	HEPES	HEPES	46.8	43.3	49.7
	CF	HEPES	46.4	44.5	48.6
		FCS	46.4	44.5	48.7
40%DPPC (TSL 40)	HEPES	HEPES	49.4	46.5	52.3
	CF	HEPES	49.5	47.1	51.4
		FCS	49.5	47.2	51.5
20% DPPC (TSL 20)	HEPES	HEPES	52.1	50.0	54.3
	CF	HEPES	52.0	50.2	54.4
		FCS	51.9	50.3	53.9
0% DPPC (TSL 0)	HEPES	HEPES	54.6	52.8	57.1
	CF	HEPES	54.2	53.6	55.9
		FCS	54.3	53.6	56.3

3.2. Pseudo-binary phase diagram of DPPC-DSPC liposomes

Based on initial and terminal temperatures of phase transition measured by DSC in Table 2, a pseudo-binary phase diagram of DPPC-DSPC liposome is plotted (Fig. 2). Lines in green are the liquidus and solidus curves of CF-TSL measured in FCS, and lines in red are for samples measured in HEPES. Almost overlapping curves were observed in both media.

3.3. Time-dependent release of CF from DPPC-DSPC formulations in FCS

DPPC-DSPC based liposome formulations with encapsulated CF were tested for triggered release in FCS at different temperatures for 600 s, respectively. Each CF release curve (Fig. 3) was fitted by the three release kinetic equations described in Section 2.5 separately to obtain the best release equation match for each formulation based on the determination coefficient R^2 (Table 3). A better coefficient of determination was obtained with the Higuchi release model when 40% or more DPPC was present in the liposomal composition. While with DPPC content equal to or lower than 20%, First order kinetics is more appropriate to describe

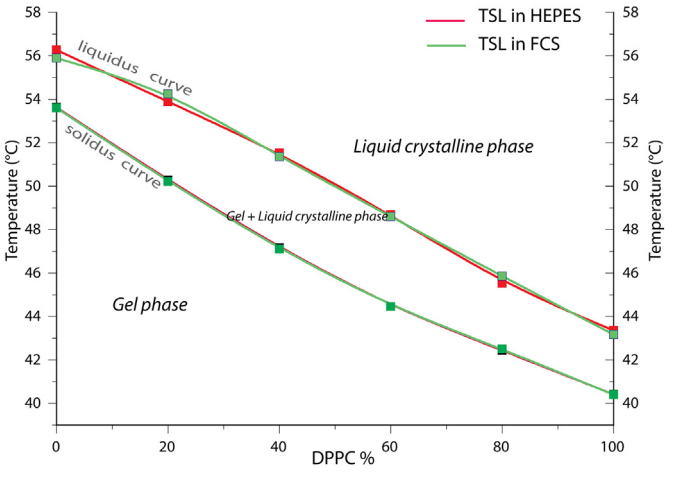

Fig. 2. Pseudo-binary phase diagram of CF TSL plotted from the initiation and completion temperatures deducted from DCS measurements in HEPES buffer (red line) and FCS (green line). Samples were formulated as DPPC-DSPC liposomes with CF loading for measurement. (For interpretation of the references to color in this figure legend, the reader is referred to the web version of this article.)

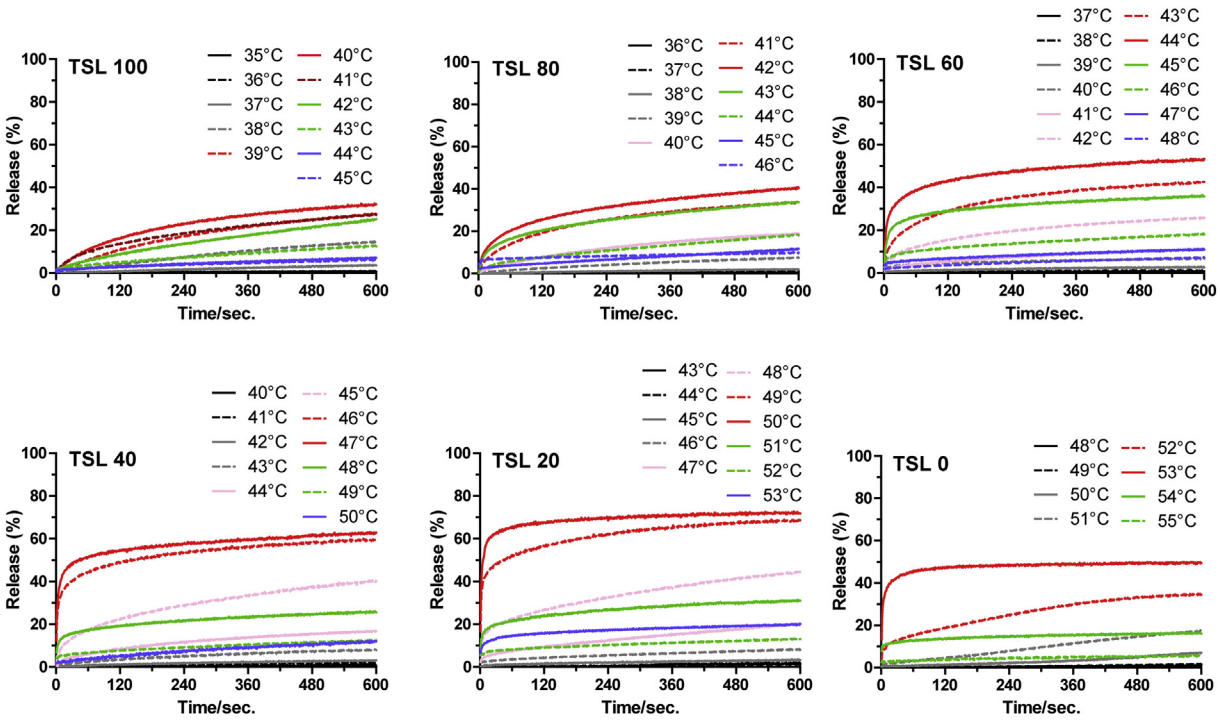

Fig. 3. CF time/temperature-dependent release in FCS from TSL100, TSL80, TSL60, TSL40, TSL20 and TSL0. 100–0 indicates the percentage of DPPC. Mean of at least three independent measurements is depicted.

CF release profiles. However, the differences between these three fitting models are minor.

3.4. Temperature-dependent release of CF from DPPC-DSPC formulations in FCS

Temperature-dependent release of the six DPPC-DSPC based liposome formulations was compared at appropriate temperature ranges (Fig. 4A). It was observed that with increasing temperature, regardless of DPPC-DSPC composition, CF release from TSLs gradually increased until reaching the maximum release temperature (Tm), and was then followed by a rapid decrease as the temperature increased further. Additionally, the maximum CF release at Tm from TSLs showed a significant improvement with lower DPPC content; the highest release reached 73 ± 4% from TSL20, while only 42 ± 6% release was observed from TSL80 at their Tm, respectively. Liposomes composed of pure DSPC or DPPC showed however a reduced release of CF compared with other binary-component liposomes during phase transition (Fig. 4A). Based on calculations with the proper fitting release equations, CF release rate constants of each formulation were computed at Tm, respectively (Table 4). As seen, k_{Tm} shows similar trend with the change of the amount of DSPC in TSL.

A CF-release pseudo-binary phase diagram of DPPC-DSPC based TSLs was plotted based on measured temperature release ranges shown in Fig. 4B, which demonstrates similar profiles with DSC based phase diagram.

Table 3
Kinetic profile of CF release from DPPC-DSPC based liposomal formulations.

	Determination coefficient R^2					
	TSL100	TSL80	TSL60	TSL40	TSL20	TSL0
Zero order	0.92797	0.91903	0.85759	0.88797	0.92630	0.94131
First order	0.91137	0.92038	0.89323	0.91025	**0.93410**	**0.94322**
Higuchi	**0.93806**	**0.95473**	**0.91194**	**0.95473**	0.92467	0.89401

Determination coefficient was determined by curve fitting of at least 3 independent experiments per formulation. Mean is depicted.

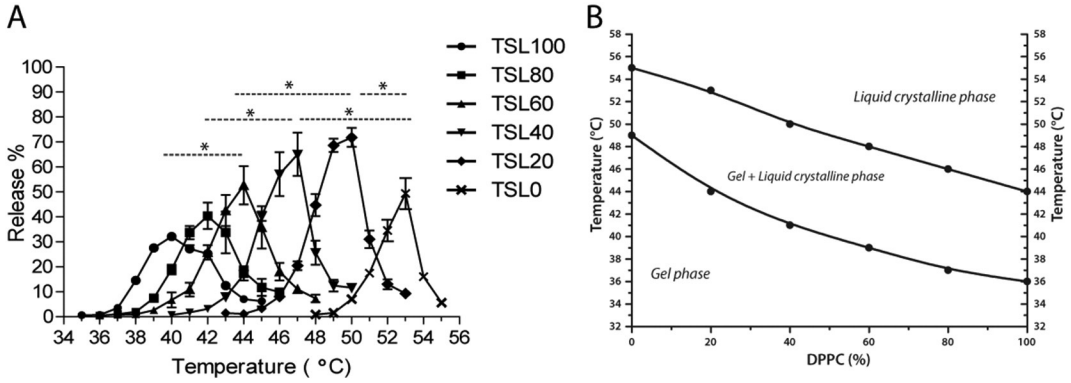

Fig. 4. A: temperature-dependent CF release from DPPC-DSPC based liposomes in FCS. Mean ± SEM are shown of at least 3 independent experiments. B: Pseudo-binary phase diagram of CF TSL plotted on the basis of CF release, in which release-starting temperature was recorded as onset of Tm and release cease-decrease temperature as the end of Tm. *Kruskal-Wallis test followed by Dunn test, p value < 0.05.

Table 4
CF release rate constants at Tm of DPPC-DSPC based liposomal formulations. Mean ± SD.

	TSL100	TSL80	TSL60	TSL40	TSL20	TSL0
k_{Tm} (10^{-4})[a]	130 ± 1 $s^{-1/2}$	290 ± 104 $s^{-1/2}$	580 ± 139 $s^{-1/2}$	640 ± 193 $s^{-1/2}$	270 ± 48 s^{-1}	140 ± 75 s^{-1}

[a] Based on determination coefficient shown in Table 3, the release rate constants k were calculated by the most fit release equation at transition temperatures of each formulation (Higuchi: TSL100–40; First order: TSL20–0) and presented as 10^{-4} $s^{-1/2}$ or 10^{-4} s^{-1}. The first 20 s of measurement at Tm were used for calculation of k [16].

3.5. Activation energy of CF release from DPPC-DSPC formulated TSLs

Based on CF release data in Fig. 4 and the Arrhenius equation, the activation energy of CF release from these different liposomal formulations was calculated (Table 4, Fig. 5). Both TSL 60 and 40 showed significantly lower activation energy for CF release, while the other formulations exhibited higher activation energy, especially in liposomes formulated by pure DPPC or DSPC lipids, suggesting that the obstruction for CF release was minimal when these binary component liposomes have a DPPC content between 40% and 60%.

3.6. The influences of PEG incorporation and PEG content on CF-TSL release

Previously we demonstrated that incorporation of more PEG-DSPE causes a higher CF leakage at phase transition [19]. We observed that 5 mol% PEG lipid in a standard formulation with DPPC-DSPC is enough to generate content release from TSLs. In order to investigate the effect of pure DPPC-DSPC TSLs composition on CF release we formulated liposomes with a minimal amount of PEG. To avoid aggregation of the nanoparticles 0.5 mol% PEG-DSPE is needed, which was added to all formulations. An obvious decreased of CF release was observed from all TSLs after reducing PEG lipid to 0.5 mol% compared to the original formulations containing 5 mol% PEG (Fig. 6). A comparable trend was observed concerning CF release at Tm which gradually increased from TSL100 (7 ± 3% vs 42 ± 6% at high PEG formulation; nonparametric Mann-Whitney test $p = 0.029$) to TSL20 (46 ± 6% vs 73 ± 4%; $p = 0.016$) when minimal PEG was applied. Interestingly, unlike other TSL formulations CF release from TSL0 seemed not to be influenced by PEG content, showing 40 ± 4% and 49 ± 10% ($p = 0.114$) release at high and low PEG formulations, respectively.

3.7. The influences of cholesterol amount on CF-TSL release

Cholesterol is commonly used in many liposomal formulations, which may however affect release kinetics profile of thermosensitive liposomes. Based on the Doxil-like formulation, we investigated CF release from TSLs composed of DSPC and 40, 20 and 10 mol% cholesterol. DSC measurements (Fig. 7A) of these TSLs displayed a gradually widened and slightly declined phase transition temperature when increasing cholesterol from 10 mol% to 20 mol% in comparison with no cholesterol contained TSL. However, no phase transition can be detected when 40 mol% cholesterol was applied. Temperature-dependent release assays confirmed these observations with absent CF release at 40 mol% cholesterol, while approximate 20% CF release was observed in formulations containing 10 and 20 mol% cholesterol formulations, both of which showed dramatic release decrease compared to the original formulation.

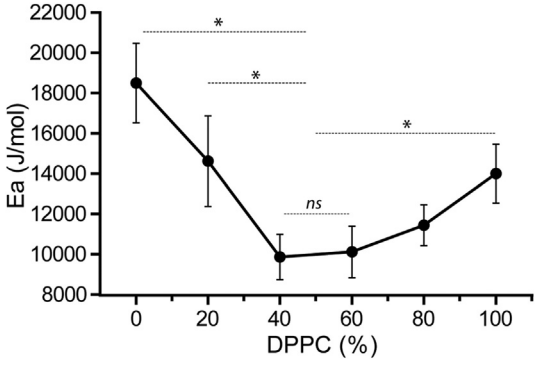

Fig. 5. Activation energy of CF release from liposomes composed of various amount of DPPC-DSPC. *Kruskal-Wallis test followed by Dunn test, p value < 0.05; *ns*, not significant at the 0.05 probability level.

4. Discussion

Here we demonstrate that bi-component DPPC-DSPC based TSLs have an optimal lipid ratio at which release rate at transition temperature is maximal. We observe that with the increase of the amount of DSPC, release rates increase as well (r_{Tm} in Table 5), and at an appropriate DPPC and DSPC ratio bi-component TSLs release significantly faster than mono-component liposomes at transition temperatures.

It is generally believed that thermosensitive liposomes exhibit the highest permeability when reaching their Tm, which causes maximum interfaces between solid and liquid phases in membranes, therefore leading to massive release of content [10]. Besides, temperature may be positively correlated to release rate [24] as the maximum release rates of these 6 formulations were measured at different and also increasingly higher transition temperatures. In order to elucidate DPPC-DSPC based TSL release kinetics, based on the general rules of diffusion release, namely Fick's first law, CF release rate can be given by:

$$r = -D * A * dC/dx = -K * T * A * dC/dx$$

where D represents the diffusion coefficient and is proportional to temperature, which can be presented as the product of temperature T and constant K in this case. A is the diffusion area of release, and dC/dx is CF concentration gradient inside and outside of the liposomal membrane, which is the same in all TSL formulations. Herein both temperature and the release area in membrane affect CF release rates. The interfaces between solid and liquid phases in membrane of each formulation, namely release areas, reach maximum at their respective Tm. When we compare the TSL release rates using the experimental data measured at the same temperature most of these TSL are not in the maximum solid-liquid interface density. In order to compare their maximum release rates and eliminate the temperature factor we used the definite integral form of the Arrhenius equation (see below) to calculate the theoretical release rates. To do so we chose a given and same temperature for all TSL formulations but maintained the maximum release areas for each TSL formulation. Thus their solid-liquid interfaces are remained as maximum as are at their respective Tm, but the temperature is unified at in this case at 42 °C to calculate the theoretical release rates of each formulation (Table 5).

$$\ln(k_{Tm}/k_{42}) = \ln(r_{Tm}/r_{42}) = Ea * (T_{max} - T_{42})/(R * T_{max} * T_{42})$$

where r_{Tm} is the CF release rate measured at Tm of each TSL formulation, which was obtained from the results in Section 3.3. Ea is the activation energy of CF release, R is the universal gas constant, and T is expressed as thermodynamic temperature in kelvin.

Release rates (r_{42}) in Table 5 show the same trend of faster CF release rates with increasing amount of DSPC in liposomes from TSL 100 to 20 but with a drop in TSL 0, implying that temperature is not the main

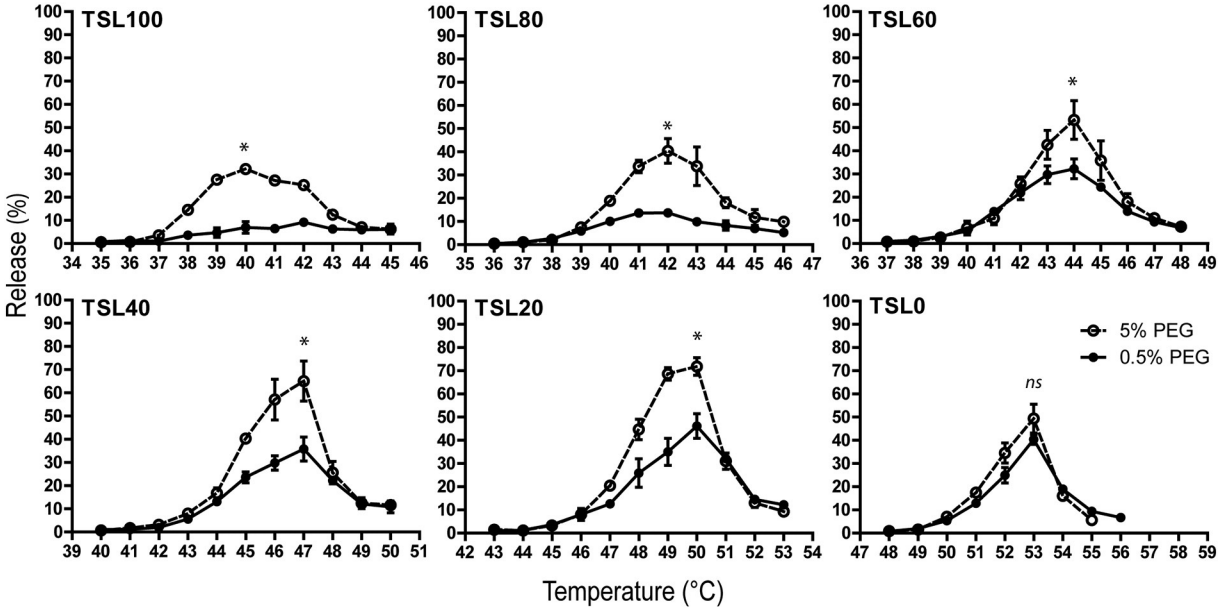

Fig. 6. Effect of PEG amount (5 mol% (open symbol) and 0.5 mol% (closed symbol)) on temperature-dependent CF release from DPPC-DSPC based liposomes in FCS. Mean ± SEM are shown of 3 or more independent experiments. *Nonparametric Mann-Whitney test, p value < 0.05; *ns*, not significant at the 0.05 probability level.

driving force that varies CF maximum-release-rates among these TSLs. We postulate that other factors intrinsic to the TSL formulation and used components determine release kinetics.

As seen in Fick diffusion equation, the increase of DSPC in TSL may increase the release area, thus leading to higher release. Hence, we hypothesize that the amount of interfaces in the liposomal membrane varies as a consequence of DPPC/DSPC ratios. The underlying mechanism we propose is that optimizing the amount of DSPC generates more solid-liquid interfaces in the membrane, increasing the release areas, thus improving CF release rate at phase transition.

Binary phase diagrams can be used to illustrate the explanation of increased release areas in DPPC-DSPC based TSLs (Figs. 2 and 4B). Unlike theoretical prediction, the experimental phase diagram did not exhibit "closed" curves in TSL 100 and 0 liposomes, which is because this is not pure bi-component system in literally. The presence of PEG lipid and interaction with serum factors as well can influence phase transition temperature of TSL 100 and 0, resulting in the deviation from the theory [25]. Fig. 2, was drawn on the basis of data measured by DSC, which reflects the macro thermodynamic behavior of lipid membrane at milligram scale. While Fig. 4B was plotted based on the amount of CF molecules released through the lipid membrane during phase transition, reflecting the detection of mesoscopic behavior at nanogram scale. Apparently, the latter is more sensitive as well as closer to reality when tracking lipid membrane phase transition, which is able to indicate the phase changes in lipid membrane earlier. Therefore, it is reasonable and reliable to illustrate liposomal thermostability on the basis of the extent of content release.

According to Fig. 4B, the molar ratios of gel and liquid phase in liposomal membranes at respective transition temperatures can be calculated by Lever Rule (Fig. 8 and Table 6).

$$\text{Lever Rule}: n_{s(\text{quantity of solids})} * L_{s(\text{distance to solidus or to Y axis})} = n_{l(\text{quantity of liquid})} * L_{l(\text{distance to liquidus or to Y axis})}$$

It was found that in TSL 60, 40 and 20 at Tm, which showed massive release, the lipid membranes were composed of nearly equal amount of gel phase and liquid crystalline phase, which may generate the maximum solid/liquid interfaces in the membranes for content release. However, around two third of the lipid membrane was in liquid crystalline state in TSL 80 at Tm, thus inducing less interfaces between solid and liquid phases, and hence diminishing CF release.

Binary-component systems are inhomogeneous during crystal nuclei formation and growth. Based on the above depicted DPPC-DSPC pseudo-binary phase diagram (Fig. 8), the composition of crystal grains is constantly changing when cooling down from liquid crystalline phase

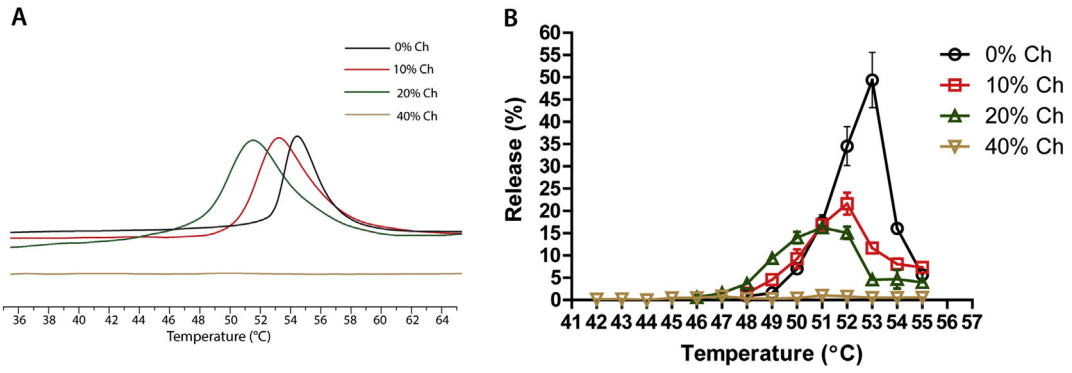

Fig. 7. DSC scans (A) and temperature-dependent release (B) of liposomes composed of 40, 20, 10 and 0 mol% cholesterol and DSPC. Results of 3 independent experiments are shown Mean ± SEM.

Table 5
CF release from different DPPC-DSPC based liposomes.

	TSL 100	TSL 80	TSL 60	TSL 40	TSL 20	TSL 0
r_{Tm} (%/min)	9.9 ± 1.3	20.4 ± 3.2	38.6 ± 14.4	51.3 ± 16.9	65.3 ± 6.9	45.1 ± 12.2
T_{max} (°C)	40	42	44	47	50	53
Ea (J/mol)	14,029	11,447	10,118	9866	14,621	18,503
r_{42} (%/min)	10.3 ± 1.3	20.4 ± 3.2	37.7 ± 14.1	48.4 ± 16.1	56.9 ± 6.0	35.5 ± 9.6

r_{Tm} (%/min): the experimentally measured CF release percentage in 1 min at maximum release temperature.
T_{max}: temperature of maximum CF release.
Ea: CF release activation energy in average.
r_{42} (%/min): the theoretically calculated CF release percentage for 1 min at 42 °C based on Arrhenius equation.
Mean ± SD, $N \geq 3$.

to gel phase. Crystal nuclei are initially formed by pure DSPC or with a little DPPC during cooling, and DPPC increasingly accumulates at the growing grains due to its lower melt point. Meanwhile solidified DSPC gradually decreases with temperature decline. For example TSL 60 in Fig. 8, when temperature declines to point E (48 °C), numerous crystal nuclei are formed as solid solution which is composed of 4.3% DPPC and 95.7% DSPC. Growing crystal grains are subsequently formed by continuous accumulation of solidified lipids to the crystal nuclei with further cooling down, of which the percentage of DPPC is gradually increased with the line F (48 °C, 4.3% DPPC) to G (39 °C, 60% DPPC). These crystal grains stop growing when touching their adjacent grains. Therefore, the content of DSPC in a crystal grain is decreases from crystal nucleus to outward region, while the content of DPPC keeps increasing. Inhomogeneous, multilayer structured crystal grains are largely formed in bi-component membranes in this way, with gradually lowered melting points from the core to the outer layers of each crystal grain.

Hence, according to analysis of the binary phase diagram we propose that a DPPC-DSPC based bi-components liposomal membrane is composed of a large amount of these inhomogeneous, nano-sized crystal grains (Fig. 9). The contact regions of these crystal grains, namely the outmost layers of crystal grains, form the crystal grain boundaries (green stripe in Fig. 9) and, are rich in DPPC, thus leading to a lower melting point in these regions compared with inner layers of crystal grains which are rich in DSPC. Consequently, a priori phase transition occurs at these boundary regions at transition temperature when heating up, which generates these crystal grains outmost layers to melt but inner layers stay solid, thus forming solid-liquid interfaces which allow content release in bi-component TSLs. However, in mono-component liposomes homogeneous crystal grains are formed

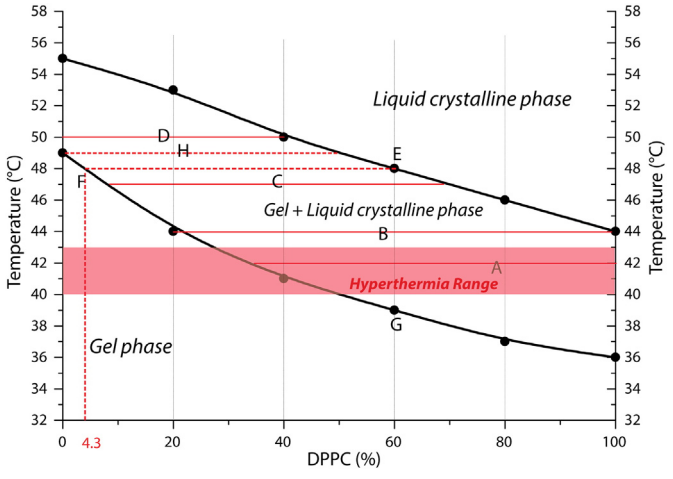

Fig. 8. Pseudo-binary phase diagram modified from Fig. 4B. A, B, C and D represent the maximum release temperatures of respective CF-TSLs and their distances to solidus and liquidus (along the drawn solid red line) were used to calculate solid/liquid phase ratios at Tm. For TSL 20, L_s is distance from D to left Y axis; from A to right Y axis is L_l for TSL 80. (For interpretation of the references to color in this figure legend, the reader is referred to the web version of this article.)

in membranes, with a homogeneous melting point from nucleus to outer region (Fig. 9). Thus, no solid-liquid interfaces are formed between crystal grains of mono-component membrane at transition temperature.

Next to the crystal grain formation, membrane defects (black stripes in Fig. 9) are formed between membrane domains due to the curved spherical liposome surface [12]. Highly disordered arrangement of lipid molecules occurs because of different lattice orientation [11], resulting in a lower melting point in these defect regions. Hence priori phase transition takes place in these regions in both bi- and mono-component TSLs at transition temperature, forming interfaces between solid and liquid phases for content release (Fig. 9). We argue that melting not only happens at defect regions but also at numerous crystal grain boundaries during phase transition. Thus bi-component membranes generate significantly increased solid-liquid interfaces than mono-component membranes, which only melt at defect regions at Tm (Fig. 9 middle row), this results in faster and more content release in bi-component TSLs. When heating above Tm, the whole liposome membrane is in a liquid phase which takes away the solid-liquid interfaces, thus evidently decreasing release as we observed in both bi- and mono-component TSLs (Fig. 9 top row).

In bi-component liposomes, however, maximum release varies significantly between TSL 60, 40 and 20. Table 5 shows almost the same solid-liquid phase ratios between these TSL 60, 40 and 20 at their maximum release temperatures, but that does not imply that the amount of interfaces between gel and liquid crystalline phases are the same. One possible explanation could be that more crystal grains are formed when liposomal membranes containing more DSPC, which hence generates more solid-liquid boundaries at transition temperatures. Another possibility is that due to the longer chain length and higher rigidity of DSPC compared to DPPC molecules, more membrane defects are generated in liposomal membranes containing more DSPC as a consequence of higher curvature stress (Fig. 9 TSL 0). We indeed observed that when the size is increased (Supplementary Fig. 1, Supplementary Table 1), lack of curvature stress in the lipid membrane caused dramatically reduced release, especially in mono-component TSLs which showed comparable extend of CF leakage (Supplementary Fig. 1 TSL 100 vs TSL 0); while bi-component TSL still demonstrated, but reduced, heat-triggered release (Supplementary Fig. 1 TSL 60).

According to the phase diagram in Fig. 8, the gel phase occupies 60% of the membrane in TSL 20 when cooling down to point H (calculated by Lever Rule). In addition, more than half of the membrane in TSL 20 is solidified and formed by pure DSPC lipids at point H, thus creating a pure DSPC-based continuous phase in membrane. While during cooling of TSL 40 and 60, the continuous phases are solid solution composed of DSPC and DPPC rather than pure DSPC. Continuous phases formed by pure DSPC structurally differ from those formed by DPPC/DSPC solid solution. This may be another reason why TSL 20 and 0, with pure DSPC as continuous phase in membranes, showed higher release than TSL 60, 40 and 100.

The activation energy of CF release (Fig. 5) gradually decreased from TSL 100 to 40, which is due to the increased number of interfaces in membranes that facilitate CF release. It requires high activation energy

Table 6
The ratios of solid and liquid phase in liposomal membranes at maximum CF release temperature of different DPPC-DSPC based liposomes.

	TSL 100	TSL 80	TSL 60	TSL 40	TSL 20	TSL 0
T_{max} (°C)	40	42	44	47	50	53
n(s):n(l) (mol/mol)	–	0.44	1.00	0.94	1.00	–

to release CF from TSL 20 and 0, which can be attributed to the enhanced hydrophobicity and thickness of the membrane as a consequence of continuous phases composed of pure DSPC lipid in TSL 20 and 0, thus needing high activation energy for CF release. However, it seems that release from areas with enhanced leakiness, as results of bending defects in membranes, supersedes the release obstruction resulting from high activation energy. Therefore TSL 20 and 0 still showed fast CF release.

Komatsu et al. demonstrated that content release from a liposomal aqueous core follows first order kinetics [27]. However, based on the determination coefficient R^2 (Table 3) resulted from fitting by three kinetic equations in Section 2.5, we found that CF release better correlates with the Higuchi model when liposome contained DPPC more than or equal to 40%. While it is proper described by the first-order release model when more than 80% of the liposomal membrane is made up by DSPC. The Higuchi model describes pore-based release models [28], which suggests that especially TSL 80–40 are likely to present a pore-like release profile during phase transition. These nano-scale pores result from the large amount of solid-liquid interfaces in bi-component membranes. While for TSL 20 and 0, due to the increase of long chain DSPC lipids in TSL the membranes become thicker, leading to increased diffusion path length for CF in membrane, thus displaying first-order release pattern [28]. Importantly, in this study the fitting differences of these TSL release profiles are not significant.

Taken together we conclude that interfaces between gel and liquid crystalline phases are crucial for massive release of content at Tm. Moreover, while typically liposomes are coated with PEG to prolong circulation time, PEG facilitates rapid release kinetics as well. PEG lipids tend to accumulate at interface areas due to their surface activity, consequently stabilizing these interfaces to release CF [9]. Therefore, when liposomes contain a low content of PEG lipids dramatically diminished CF release was observed (Fig. 6). The lack of such an effect in TSL 0 may be because the resulting interfaces in TSL 0 are more rigid due to pure DSPC composition, thereby more stable interfaces are generated in TSL 0 membranes enabling CF release even without help of PEG. Additionally, PEG lipid (DSPE-PEG) has the same lipid moiety as DSPC rather than DPPC, which could also explain the significant decreased release in TSL 100 containing lower PEG lipids. Cholesterol is applied to improve the stability of liposomal membranes, but it also maintains a certain degree of fluidity of the membrane above as well as below Tm [29]. Through this action cholesterol passivates the response of TSL membrane to transition temperature by inserting between lipid molecules which affects inter-molecular ordered arrangement of phospholipids in the membrane [23,29]. As a result, we think, cholesterol molecules obscure membrane defects and boundaries, leading to less or no interfaces

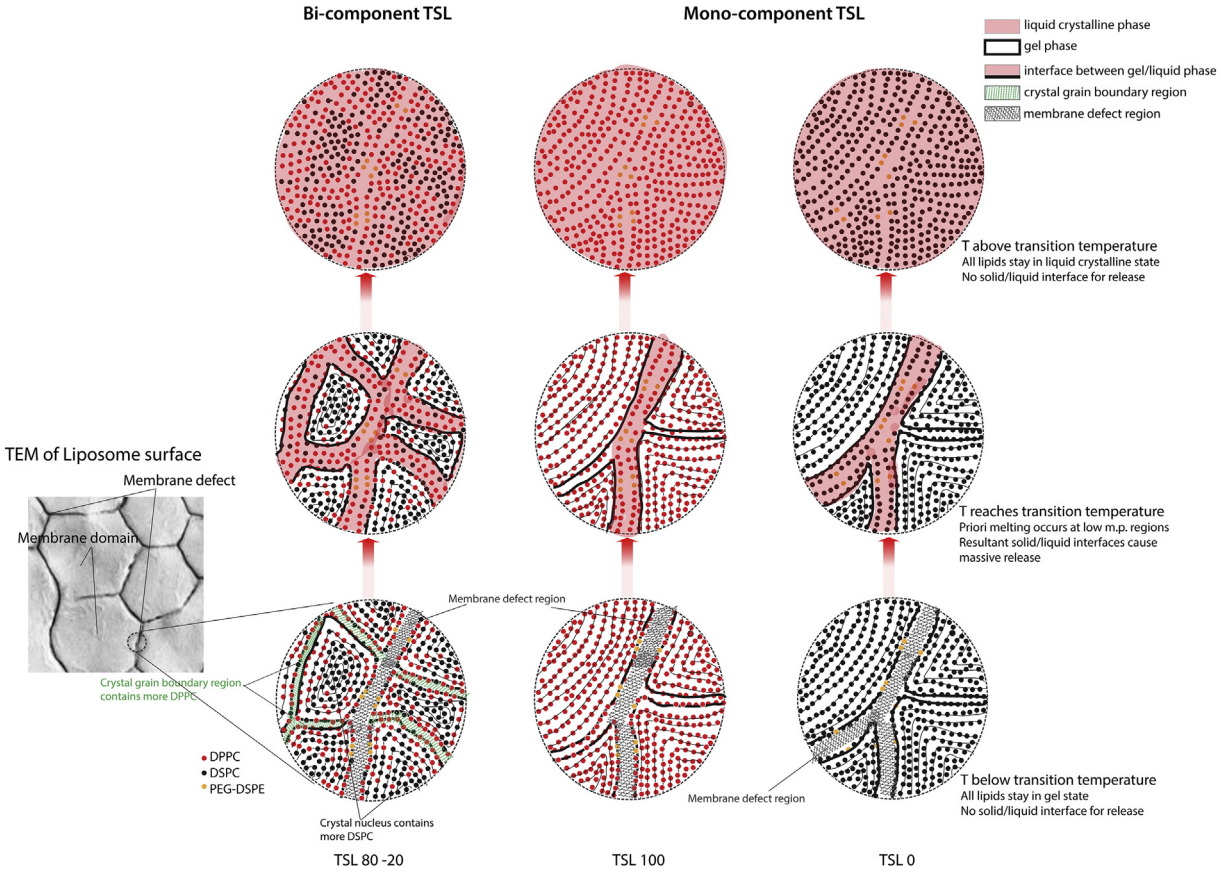

Fig. 9. Crystal grains in bi-component liposomal membranes are formed as inhomogeneous microstructures with lower melting point in the outer layer, while mono-component crystal grains in a homogenous (i.e. mono-component) structure have the same melting point across the grains. In membrane defect regions the melting point is also lower. At transition temperatures, both grain boundary (green stripe) and defect (black stripe) regions melt (pink) in bi-component TSLs, whereas only membrane defect regions melt in mono-component TSLs at transition temperatures, thus creating less gel/liquid interfaces for content release in TSL 100 and 0. When above transition temperatures, all TSLs are in pure liquid phase, thus no interfaces for release are present. The transmission electron microscopy graph of lipid membrane is cited from paper of Landon et al. [26] and authorized by the publisher. (For interpretation of the references to color in this figure legend, the reader is referred to the web version of this article.)

during phase transition. In addition, incorporation of cholesterol increases the membrane lipophilicity and therefore barrier function to hydrophilic compounds which likely explains the remarkable decrease of CF release and declined thermosensitivity as observed in cholesterol containing liposomes (Fig. 7).

Considering the applicable hyperthermia range in the clinic (40–43 °C), a DPPC content has to be selected which balances instability with rapid release. TSLs with a DPPC content above 80% are prone to leak at around physiological temperature because the membrane already goes through phase transition at 37 °C (Fig. 8). The onset of phase transition of liposomes with a DPPC content of 40% or lower on the other hand, starts at 41 °C, with only a minor fraction of the lipids convert to a liquid state. Based on Level Rule, the percentage of liquid crystalline phase in the membrane at this state is still low (~17%) even at 43 °C, thus generating lesser interfaces for release. Therefore, in DPPC-DSPC based thermosensitive liposomes the amount of DPPC should be above 40% and not beyond 80% for a fast triggered drug release at a preferred hyperthermia temperature.

5. Conclusion

Thermosensitive liposomes are promising delivery systems for solid tumor treatment combined with local hyperthermia. It is crucial that TSLs display rapid content release when exposed to the right temperature, generating a steep drug gradient which benefits subsequent tumor uptake. The present work, based on the analysis of phase equilibrium, illustrates that inhomogeneous crystal grains consisting membranes form in DPPC-DSPC bi-component TSLs. These inhomogeneous microstructurally organized membranes offer numerous solid-liquid phase interfaces, namely nano-scale gaps, at transition temperature at crystal grain boundaries and defect regions, enabling rapid release. These induced nano-scale gaps in liposome membranes are adjustable in quantity by changing DPPC and DSPC ratios, thus presenting different release kinetics, which can be used to further develop TSLs for wider application in the clinic.

Acknowledgements

We thank Dr. Lars Lindner at Ludwig-Maximilians-University of Munich, for kindly providing purified carboxyfluorescein in powder.

Appendix A. Supplementary data

Supplementary data to this article can be found online at http://dx.doi.org/10.1016/j.jconrel.2016.12.030.

References

[1] Y. Matsumura, H. Maeda, A new concept for macromolecular therapeutics in cancer chemotherapy; mechanism of tumoritropic accumulation of proteins and the antitumor agent SMANCS, Cancer Res. 46 (1986) 6387–6392.
[2] X.L. Cun, J.T. Chen, S.B. Ruan, L. Zhang, J. Wan, Q. He, H.L. Gao, A novel strategy through combining iRGD peptide with tumor-microenvironment-responsive and multistage nanoparticles for deep tumor penetration, ACS Appl. Mater. Interfaces 7 (2015) 27458–27466.
[3] H. Cabral, Y. Matsumoto, K. Mizuno, Q. Chen, M. Murakami, M. Kimura, Y. Terada, M.R. Kano, K. Miyazono, M. Uesaka, N. Nishiyama, K. Kataoka, Accumulation of sub-100 nm polymeric micelles in poorly permeable tumours depends on size, Nat. Nanotechnol. 6 (2001) 815–823.
[4] S.K. Hobbs, W.L. Monsky, F. Yuan, W.G. Roberts, L. Griffith, V.P. Torchilin, R.K. Jain, Regulation of transport pathways in tumor vessels: role of tumor type and microenvironment, Proc. Natl. Acad. Sci. 95 (1998) 4607–4612.
[5] A.L.B. Seynhaeve, S. Hoving, D. Schipper, C.E. Vermeulen, G. aan de Wiel-Ambagtsheer, S.T. van Tiel, A.M.M. Eggermont, T.L.M. ten Hagen, Tumor necrosis factor α mediates homogeneous distribution of liposomes in murine melanoma that contributes to better tumor response, Cancer Res. 67 (2007) 9455–9462.
[6] M.B. Yatvin, J.N. Weinstein, W.H. Dennis, R. Blumenthal, Design of liposomes for enhanced local release of drugs by hyperthermia, Science 202 (1978) 1290–1293.
[7] G. Kong, M.W. Dewhirst, Hyperthermia and liposomes, Int. J. Hyperth. 15 (1999) 345–370.
[8] D. Needham, G. Anyarambhatla, G. Kong, M.W. Dewhirst, A new temperature sensitive liposome for use with mild hyperthermia: characterization and testing in a human tumor xenograft model, Cancer Res. 60 (2000) 1197–1201.
[9] D. Needham, J.Y. Park, A.M. Wright, J.H. Tong, Materials characterization of the low temperature sensitive liposome (LTSL): effects of the lipid composition (lysolipid and DSPE PEG2000) on the thermal transition and release of doxorubicin, Faraday Discuss. 161 (2013) 515–534.
[10] B. Kneidl, M. Peller, G. Winter, L.H. Lindner, M. Hossann, Thermosensitive liposomal drug delivery systems: state of the art review, Int. J. Nanomedicine 9 (2014) 4387–4398.
[11] L.M. Ickenstein, M.C. Arfvidssonc, D. Needhamd, L.D. Mayera, K. Edwards, Disc formation in cholesterol-free liposomes during phase transition, Biochim. Biophys. Acta 1614 (2003) 135–138.
[12] A.G. Lee, Functional properties of biological membranes: a physical–chemical approach, Prog. Biophys. Mol. Biol. 29 (1975) 3–56.
[13] J.K. Mills, D. Needham, Lysolipid incorporation in dipalmitoylphosphatidylcholine bilayer membranes enhances the ion permeability and drug release rates at the membrane phase transition, Biochim. Biophys. Acta 1716 (2005) 77–96.
[14] T. Tagami, M.J. Ernsting, S.D. Li, Optimization of a novel and improved thermosensitive liposome formulated with DPPC and a Brij surfactant using a robust in vitro system, J. Control. Release 154 (2011) 290–297.
[15] M.H. Gaber, K. Hong, S.K. Huang, D. Papahadjopoulos, Thermosensitive sterically stabilized liposomes: formulation and in vitro studies on mechanism of doxorubicin release by bovine serum and human plasma, Pharm. Res. 12 (1995) 1407–1416.
[16] M. Hossann, M. Wiggenhorn, A. Schwerdt, K. Wachholz, N. Teichert, H. Eibl, R.D. Issels, L.H. Lindner, In vitro stability and content release properties of phosphatidylglyceroglycerol containing thermosensitive liposomes, Biochim. Biophys. Acta 1768 (2007) 2491–2499.
[17] L.H. Lindner, M.E. Eichhorn, H. Eibl, N. Teichert, M. Schmitt-Sody, M. Dellian, Novel temperature-sensitive liposomes with prolonged circulation time, Clin. Cancer Res. 10 (2004) 2168–2178.
[18] F. Guo, M. Yu, J.P. Wang, F.P. Tan, N. Li, Smart IR780 theranostic nanocarrier for tumor-specific therapy: hyperthermia-mediated bubble-generating and folate-targeted liposomes, ACS Appl. Mater. Interfaces 7 (2015) 20556–20567.
[19] L. Li, T.L.M. ten Hagen, D. Schipper, T.M. Wijnberg, G.C. van Rhoon, A.M. Eggermont, L.H. Lindner, G.A. Koning, Triggered content release from optimized stealth thermosensitive liposomes using mild hyperthermia, J. Control. Release 143 (2010) 274–279.
[20] L. Li, T.L.M. ten Hagen, M. Hossann, R. Suss, G.C. van Rhoon, A.M. Eggermont, D. Haemmerich, G.A. Koning, Mild hyperthermia triggered doxorubicin release from optimized stealth thermosensitive liposomes improves intratumoral drug delivery and efficacy, J. Control. Release 168 (2013) 142–150.
[21] T. Lu, W.J.M. Lokerse, A.L.B. Seynhaeve, G.A. Koning, T.L.M. ten Hagen, Formulation and optimization of idarubicin thermosensitive liposomes provides ultrafast triggered release at mild hyperthermia and improves tumor response, J. Control. Release 220 (2015) 425–437.
[22] W.J.M. Lokerse, E.C.M. Kneepkens, T.L.M. ten Hagen, A.M.M. Eggermont, H. Grull, G.A. Koning, In depth study on thermosensitive liposomes: optimizing formulations for tumor specific therapy and in vitro to in vivo relations, Biomaterials 82 (2016) 138–150.
[23] G.A. Hughes, Nanostructure-mediated drug delivery, Nanomed.: Nanotechnol., Biol. Med. 1 (2005) 22–30.
[24] R.A. Demel, S.C. Kinsky, C.B. Kinsky, L.L.M. van Deenen, Biochim. Biophys. Acta 150 (1968) 655–665.
[25] S. Mabrey, J.M. Sturtevant, Investigation of phase transitions of lipids and lipid mixtures by sensitivity differential scanning calorimetry, Proc. Natl. Acad. Sci. 73 (1976) 3862–3866.
[26] C.D. Landon, J.Y. Park, D. Needham, M.W. Dewhirst, Nanoscale drug delivery and hyperthermia: the materials design and preclinical and clinical testing of low temperature-sensitive liposomes used in combination with mild hyperthermia in the treatment of local cancer, Open Nanomed. J. 1 (2011) 38–64.
[27] H. Komatsu, S. Okada, Increase permeability of phase-separated liposomal membranes with mixtures of ethanol-induced interdigitated and non-interdigitated structures, Biochim. Biophys. Acta 1237 (1995) 169–175.
[28] G. Singhvi, M. Singh, Review: in-vitro drug release characterization models, Int. J. Pharm. Stud. Res. 2 (2011) 77–84.
[29] L. Coderch, J. Fonollosa, M. De Pera, J. Estelrich, A. De La Maza, J.L. Parra, Influence of cholesterol on liposome fluidity by EPR relationship with percutaneous absorption, J. Control. Release 68 (2000) 85–95.